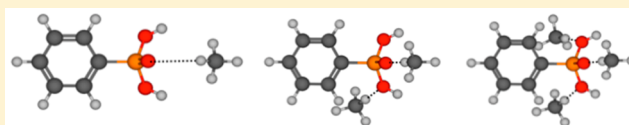


Effective Binding of Methane Using a Weak Hydrogen Bond

Alice Henley, Michelle Bound, and Elena Besley*

School of Chemistry, University of Nottingham, University Park, Nottingham NG7 2RD, U.K.

ABSTRACT: The weak hydrogen bond is an important type of noncovalent interaction, which has been shown to contribute to stability and conformation of proteins and large biochemical membranes, stereoselectivity, crystal packing, and effective gas storage in porous materials. In this work, we systematically explore the interaction of methane with a series of functionalized organic molecules specifically selected to exhibit a weak hydrogen bond with methane molecules. To enhance the strength of hydrogen bond interactions, the functional groups include electron-enriched sites to allow sufficient polarization of the C–H bond of methane. The binding between nine functionalized benzene molecules and methane has been studied using the second order Møller–Plesset perturbation theory to reveal that benzenesulfonic acid ($C_6H_5-SO_3H$) and phenylphosphonic acid ($C_6H_5-PO_3H_2$) have the greatest potential for efficient methane capture through hydrogen bonding interactions. Both acids exhibit efficient binding potential with up to three methane molecules. For additional insight, the atomic charge distribution associated with each binding site is presented.

Binding of Methane to $C_6H_5PO_3H_2$ (Phenylphosphonic Acid)

without creating sites that are difficult and expensive to regenerate.¹⁵ Examples of the weak hydrogen bond include C–H \cdots O interactions, where the hydrogen atom forms a bond between two moieties of which one or even both are of moderate to low negativity, and C–H \cdots π interactions in π electron rich molecules.¹⁶ IUPAC has previously discussed extending the definition of the hydrogen bond to include any attractive interaction X–H \cdots Y–Z, where some evidence of bond character exists between H and Y moieties, and X is more electronegative than H, even if only moderately (in the case of X as carbon).¹⁷ Within this definition, X–H is the donor and Y is the acceptor. The H \cdots Y distance is generally 2–3 Å, and 30–80% of weak hydrogen bonds have an H \cdots Y distance of less than the sum of the van der Waal radii of H and Y species. This often makes weak hydrogen bond interactions difficult to distinguish. The X–H \cdots Y angle is optimized at 180° but typically ranges from 90° to 180°, and the H \cdots Y–Z angle is optimized where the Y lone pair is directed at the hydrogen atom, or where maximum charge transfer occurs. The hydrogen bond character has been also shown in C–H/ π interactions, which play an important role in many fields that include crystals,¹⁸ conformational analysis,^{19,20} organic reactions,^{21,22} and molecular recognition.^{23–25} C–H/ π interactions govern the stability of biological structures where they affect both binding affinity and conformation. In these studies, it is also customary to use methane as the simplest model of an aliphatic compound.

INTRODUCTION

Natural gas, composed primarily of methane, is an energy-intensive fuel source that has a high molar energy density, exhibits cleaner combustion when compared to diesel or petroleum,^{1,2} and requires low utilization costs. However, due to the low energy density of methane in gaseous phase, storage of natural gas at ambient temperatures and pressures remains a real challenge limiting its industrial application potential. One promising gas storage method involves packing fuel tanks with porous material to adsorb the natural gas. This exploits weak van der Waals interactions between methane and the pore walls to achieve a density comparable to compressed natural gas but allowing ambient temperatures and moderate pressures (typically 35 bar) in less bulky fuel tanks. Several types of porous materials are being investigated and evaluated for this application including activated carbons, porous organic polymers, and metal–organic frameworks.^{3–10} Attachment of carefully selected functional groups can, in principle, enhance the interactions between methane and the pore walls to increase the packing density of methane at low pressures. Computational studies of the binding of guest molecules with functionalized ligands at the atomic scale^{11–14} have shown that finding favorable adsorption sites in the organic ligands holds a key to enhancing the ability of porous materials to capture gases. Torrisi et al.,¹² for example, showed that aromatic rings functionalized by certain groups can enhance the intermolecular interaction in different ways: methyl groups increase the inductive effect, lone-pair donating groups promote acid–base type interactions, and hydrogen bonding occurs in acidic proton containing groups.

Weak hydrogen bonds comprise a class of hydrogen bonds (HB) with typical values of the binding energy less than 17 kJ mol^{−1} (or 4 kcal mol^{−1}) but greater than the van der Waals limit of 1 kJ mol^{−1} (or 0.25 kcal mol^{−1}). This type of weak interaction allows the enhancement of affinity for methane

The primary aim of this work is to aid the selection and targeted design of functionalized organic molecules for their ability to coordinate with one or more methane molecules via weak hydrogen bond interactions. The considered molecular

Received: April 1, 2016

Revised: May 3, 2016

Published: May 5, 2016

complexes use an oxygen atom as the binding site for the methane molecule, and X—H exists as a C—H bond in methane and so is classed as a weak donor. To maximize the strength of the hydrogen bond interaction, the organic linkers were selected to ensure that the Y—Z moiety is a strong acceptor, e.g., O=C.

COMPUTATIONAL METHODS

Optimized geometries and binding energies for the functional groups supported by an aromatic or cyclohexane ring with

Table 1. Benchmarking RI-MP2, MP2, and CCSD(T) Calculations for a Model Formaldehyde–Methane Dimer

geometry optimization, level of theory/basis set	distance between H(CH ₄) and O(CH ₂ O), in Å	binding energy, level of theory/basis set	binding energy, in kJ mol ⁻¹
RI-MP2/cc-pVDZ	2.54	RI-MP2/cc-pVDZ	-0.91
		MP2/cc-pVQZ	-2.20
MP2/cc-pVDZ	2.54	MP2/cc-pVDZ	-0.91
		MP2/cc-pVQZ	-2.20
MP2/cc-pVQZ	2.61	MP2/cc-pVQZ	-2.21
CCSD(T)/cc-pVDZ	2.99	CCSD(T)/cc-pVDZ	-0.95
		CCSD(T)/cc-pVQZ	-2.24

methane were calculated for nine methane–ligand complexes using the Q-Chem quantum chemistry package.²⁶ The carbon and hydrogen atoms within the ring of the linker were fixed upon geometry optimization leaving the atoms of the functional group and the methane molecule free to find the minimum energy configurations. In the dimer, trimer, and tetramer configurations, geometry optimization was obtained using the resolution of identity MP2 level of theory (RI-MP2) with the cc-pVDZ basis set, and the binding energies were calculated at the MP2 level using cc-pVQZ basis set and the Boys and Bernardi counterpoise correction.²⁷ Partial charges on each

atom were obtained using the CHELPG scheme developed by Breneman and Wiberg.²⁸

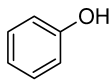
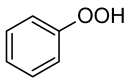
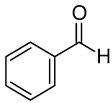
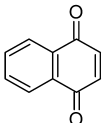
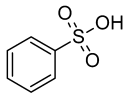
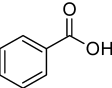
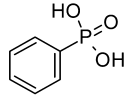
Benchmarks for the equilibrium structure and binding energy of a small formaldehyde–methane dimer are presented in Table 1 to show that the adopted computational approach is comparable in accuracy with the CCSD(T) method for the binding energies. Unlike the computationally expensive CCSD(T) method, the adopted computational approach can be used to study larger (tetramer) systems without compromising the accuracy of predictions. Table 1 shows that the MP2/cc-pVQZ binding energies calculated for the structures optimized at the RI-MP2/cc-pVDZ and MP2/cc-pVDZ levels of theory are in good agreement with those predicted directly from the MP2/cc-pVQZ equilibrium structure. The CCSD(T)/cc-pVQZ binding energy obtained for the dimer optimized at the CCSD(T)/cc-pVDZ level of theory also has a very close value.

The linker candidates presented in Table 2, all containing oxygen to create a strong hydrogen bond acceptor, were tested for their ability to bind methane. Functional groups with more than one accepting site were tested on their ability to form trimer and tetramer structures by including additional methane molecules.

RESULTS AND DISCUSSION

Figure 1 shows the lowest energy dimer configurations between methane and phenol, benzaldehyde, or cyclohexanone molecule. For the phenol–methane dimer (Figure 1a), the lowest energy conformation corresponds to the interaction between the hydroxyl group on phenol and methane where the C–H bond of methane is pointing directly to the lone pair of the oxygen atom, with the C–O⋯H being in the plane of the ring. The binding energy has a moderate value of -3.17 kJ mol⁻¹, the C–H⋯O angle is found to be 180°, and the intermolecular H(CH₄)⋯O distance is 2.58 Å. In this dimer, the interacting hydrogen of methane carries a small positive charge of +0.16 *me* and both the oxygen and the C(CH₄) become more

Table 2. Selection of Functionalized Organic Molecules Screened for Efficient Methane Binding Using a Weak Hydrogen Bond

Label	Functional group	Structure	Label	Functional group	Structure
A	C ₆ H ₅ -OH phenol		F	C ₆ H ₅ -OOH phenyl hydroperoxide	
B	C ₆ H ₅ -C(=O)-H benzaldehyde		G	C ₁₀ H ₆ O ₂ 1,4-naphthoquinone	
C	C ₆ H ₁₁ =O cyclohexanone		H	C ₆ H ₅ -SO ₃ H benzenesulfonic acid	
D	C ₆ H ₅ -COOH benzoic acid		I	C ₆ H ₅ -PO ₃ H ₂ phenylphosphonic acid	
E	C ₆ H ₅ -NO ₂ nitrobenzene				

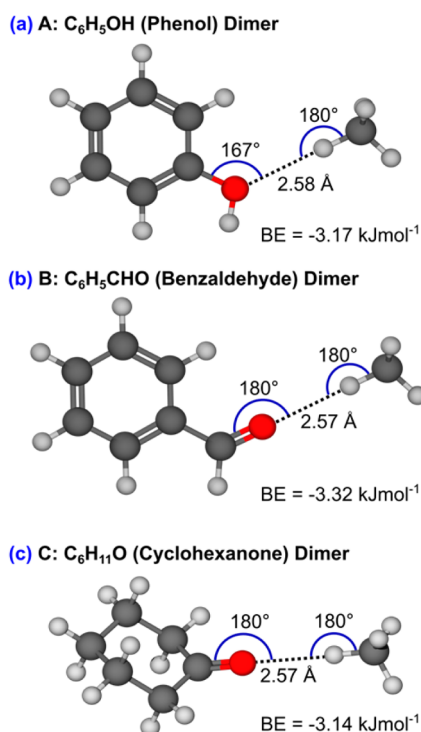


Figure 1. Dimer configurations for C_6H_5OH (phenol)– CH_4 (a), C_6H_5CHO (benzaldehyde)– CH_4 (b), and $C_6H_{11}O$ (cyclohexanone)– CH_4 (c). The sites showing the strongest binding energies (BE) with methane are found to be hydroxyl (a), aldehyde (b), and ketone (c) groups. The atoms shown in gray, white, and red represent carbon, hydrogen, and oxygen, respectively.

negatively charged upon binding. The above description indicates a typical HB-like, cohesive interaction. In the benzaldehyde–methane dimer (Figure 1b), the strongest interaction was found to be between the formyl substituent functional group attached to a phenyl ring and the methane molecule where the $C-H\cdots O=C$ atoms are located along a straight line, with the $H_{(CH_4)}\cdots O_{(O=C)}$ distance of 2.57 Å being shorter than the sum of the van der Waal radii of hydrogen and oxygen. A binding energy of -3.32 kJ mol^{-1} is comparable to that for the phenol–methane dimer shown in Figure 1a. A ketone functional group represents a binding site similar in strength and nature to the formyl group. This has been demonstrated in Figure 1c, showing the cohesive interaction between cyclohexanone and methane. This dimer has the $H-C$ bond of the methane pointing at the carbonyl oxygen such that the $C-H\cdots O=C$ atoms are aligned along a straight line. In this configuration, there is very little steric repulsion due to the way the carbonyl fixes the shape of the aliphatic ring. The moderate binding energy is expected of the carbonyl species due to the electron donating effect of the ring.

For the benzoic acid molecule, two dimer and one trimer complexes have been identified, as shown in Figure 2a–c. In dimer I the methane molecule interacts with the carbonyl-type oxygen atom via a weak HB-like interaction. Similar to the benzaldehyde–methane dimer (Figure 1b), the $C-H\cdots O=C$ interaction occurs linearly along the same axis, in the plane of the phenyl ring. The short intermolecular distance of 2.55 Å agrees with the moderate binding energy of -3.75 kJ mol^{-1} . However, in the benzoic acid–methane dimer I the carbonyl oxygen atom is involved in two weak HB interactions, making it a bifurcated HB acceptor and limiting the flexibility of rotation

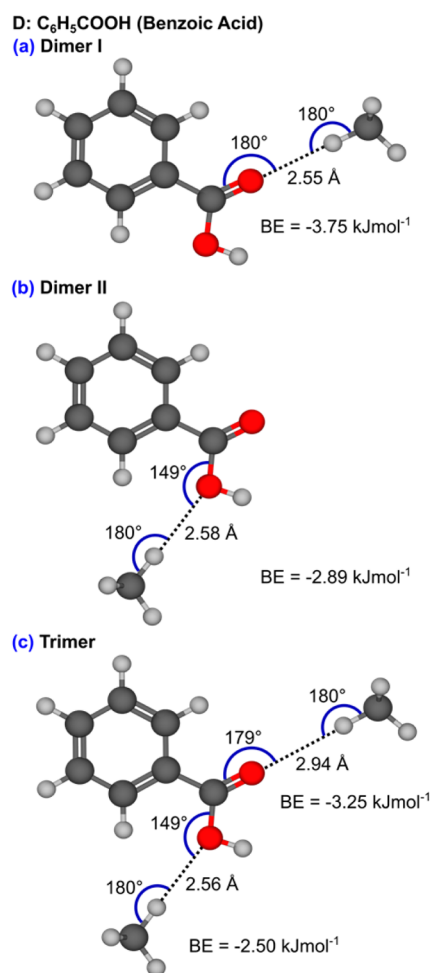


Figure 2. C_6H_5COOH (benzoic acid)– CH_4 complexes: dimer configurations I (a) and II (b), where methane binds at one of the two oxygen sites, and a trimer complex (c), where methane binds at both oxygen sites.

about the $C-OH$ bond. Dimer II of this complex involves the methane molecule interacting directly with the OH oxygen site. In this case, the $O_{(OH)}\cdots H-C$ atoms are located on the same axis and the $C-O\cdots H$ angle of 149° suggests that the lone pair of the oxygen atom is somewhat unavailable to the methane in this configuration. The interatomic distance is short, at 2.58 Å, but the binding energy remains weak, having the value of -2.89 kJ mol^{-1} despite the $O_{(OH)}$ having a more negative charge than the $O_{(C=O)}$ in the functionalized benzene. Although the binding is weaker in dimer II than in dimer I, both interactions are accompanied by an increase in positive charge at the hydrogen atom and an increase in negative charge at both the $C_{(CH_4)}$ and O atoms. Superimposing the two dimer structures gives a trimer configuration similar to that of the separate dimers but with both interactions weakened, as indicated by a significant lengthening of the $O_{(C=O)}\cdots H_{(CH_4)}$ distance to 2.94 Å and a decrease in both values for the binding energy. Despite the interaction at the carbonyl group occurring at a larger distance than the sum of the van der Waals radii of oxygen and hydrogen, the optimized geometry suggests a very directional interaction toward the oxygen lone pair symptomatic of an HB.

In the nitrobenzene–methane complex, only one dimer was tested due to the symmetry of the functional group, which gave a conformation in which the $C-H$ bond of the methane directs

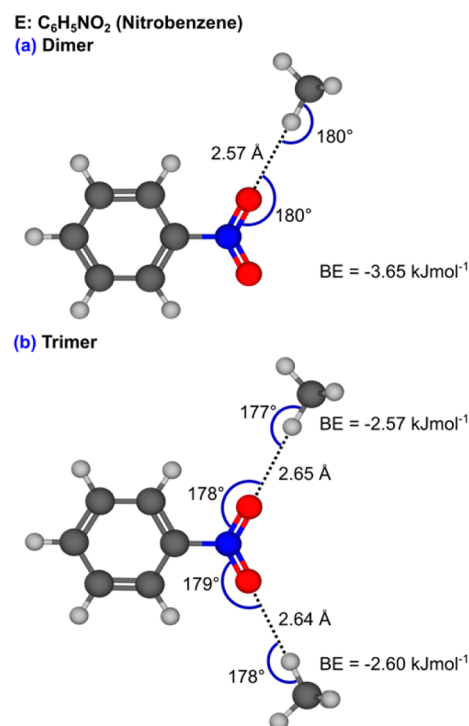


Figure 3. C₆H₅NO₂ (nitrobenzene)–CH₄ complexes: dimer (a) and trimer (b). The atoms shown in gray, white, blue, and red represent carbon, hydrogen, nitrogen, and oxygen, respectively.

to the N–O bond giving a H_(CH₄)⋯O_(NO) distance of 2.57 Å (Figure 3a). The binding energy of $-3.65 \text{ kJ mol}^{-1}$ is comparable to that of the benzoic acid dimer I shown in Figure 2a and is moderate as expected of a highly polarizing group such as $-\text{NO}_2$. Introducing another methane molecule to the system at another available oxygen site gives the trimer structure shown in Figure 3b. Upon forming the trimer, both methane molecules distance from the accepting oxygen atoms and the binding becomes slightly weaker. The binding energies are smaller than expected of a formally negatively charged oxygen.

The interaction of methane with the peroxide functionalized benzene (phenyl hydroperoxide) results in two dimer and one trimer complexes. In dimer I presented in Figure 4a the methane interacts with the oxygen atom closest to the phenyl ring. The C–H bond of the methane points to the lone pair of the oxygen nearest the ring such that the O_(C–O)⋯H–C atoms are in the plane of the ring with an intermolecular distance of 2.57 Å. The peroxide bond, however weak, serves as a good accepting site due to the electron rich nature of the adjacent oxygen atoms. The binding resulted in a significant increase of charge to -15.2 me on the methane molecule. Dimer II shown in Figure 4b has the methane interacting with the oxygen atom furthest from the phenyl ring. In this weaker dimer the methane molecule is located above the plane of the phenyl ring with the methane C–H bond positioned toward the lone pair of the accepting oxygen, thus acting as a bifurcated HB acceptor with an O_(OH)⋯H_(CH₄) distance of 2.58 Å. The H_(O–H) atom rests

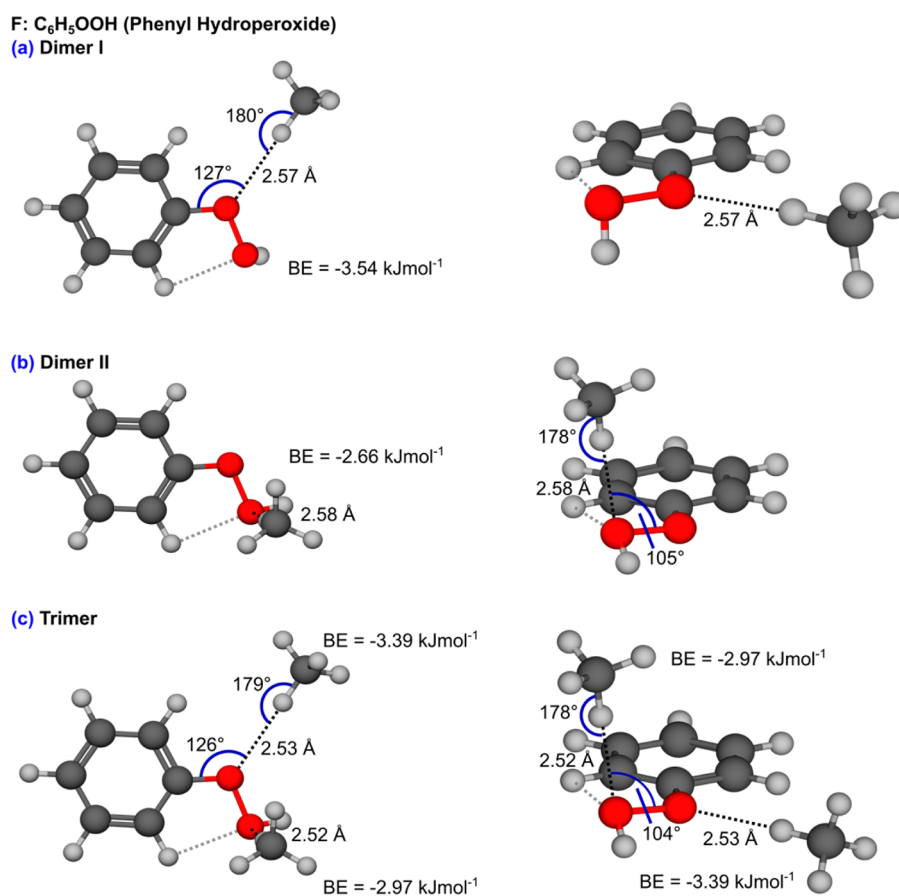


Figure 4. C₆H₅–OOH (phenyl hydroperoxide)–CH₄ complexes: dimer configurations I (a) and II (b), where methane binds at one of the two oxygen sites, and a trimer complex (c), where methane binds at both oxygen sites.

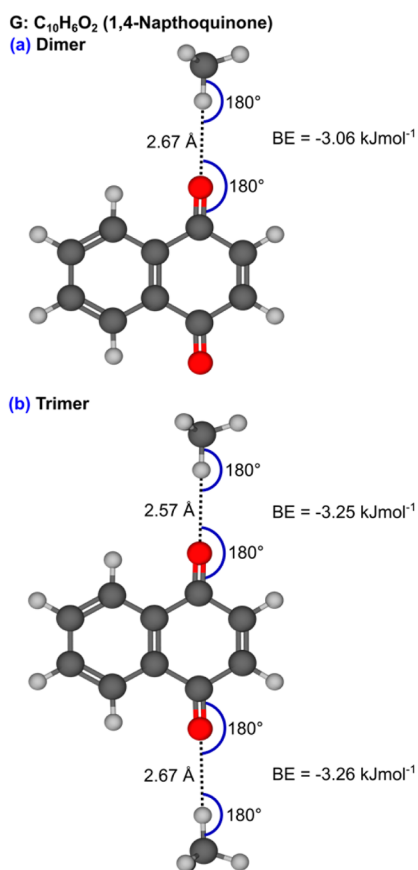


Figure 5. $C_{10}H_6O_2$ (1,4-naphthoquinone)– CH_4 complexes: dimer (a) and trimer (b).

just under the plane of the ring. Despite the $O_{(OH)}$ being more negatively charged than the $O_{(C=O)}$ atom, methane binds more weakly at the $O_{(OH)}$ atom (the binding energy of $-2.66 \text{ kJ mol}^{-1}$) than at the $O_{(C=O)}$ atom (the binding energy of $-3.54 \text{ kJ mol}^{-1}$). This is thought to be due to the $O_{(OH)}$ atom acting as a bifurcated HB acceptor. Superimposing dimers I and II form a trimer structure with moderately strong interactions at each accepting site (Figure 4c). Both methane molecules come closer to the functional group, each giving intermolecular distances of $2.52\text{--}2.53 \text{ \AA}$. The binding energy at the $O_{(OH)}$ site increased but the binding energy at the $O_{(C=O)}$ site decreased slightly.

1,4-Naphthoquinone is the largest and one of only two nonfully aromatic species tested. The dimer form shows only one oxygen atom accepting a weak HB but the trimer exhibits both available oxygen atoms involved with methane molecules. These complexes can be viewed in Figure 5a,b. In the dimer, a moderately strong interaction with a relatively long intermolecular distance of 2.67 \AA between the carbonyl oxygen and the methane hydrogen was found, giving a binding energy of $-3.06 \text{ kJ mol}^{-1}$. A marginal charge gain of -2.69 me on the methane molecule occurred upon dimer formation. Due to the symmetry of the structure, it was unnecessary to test dimer formation at the other oxygen site. As expected, upon forming the trimer the binding energies of each interaction are predicted to be similar, having the values of -3.25 and $-3.26 \text{ kJ mol}^{-1}$. The $H_{(CH_4)} \cdots O_{(C=O)}$ distances vary by 0.1 \AA , but this results in little effect on the binding.

The sulfonic acid group has three oxygen atoms available to accept a HB interaction from a methane molecule, and the

functional group is flexible across many of its bonds. There is a weak hydrogen bond within the linker itself, it exists as $O\text{--}H \cdots O=S$ and so one $S=O$ bond is involved in this interaction whereas the other is not. The complexes tested encompassing the benzenesulfonic acid molecule are shown in Figure 6. Dimer I shown in Figure 6a involves the methane interacting with the oxygen not inherently exhibiting a weak HB within the functional group. It shows a moderately strong interaction with the binding energy of $-3.16 \text{ kJ mol}^{-1}$ and an intermolecular distance of 2.53 \AA . In dimer II (Figure 6b) the methane interacts with the $S\text{--}OH$ type oxygen atom. This weaker dimer with the binding energy of $-2.79 \text{ kJ mol}^{-1}$ shows a strongly directional interaction toward the lone pair of the $O_{(OH)}$ atom at a $O_{(OH)} \cdots H_{(CH_4)}$ distance of 2.58 \AA . Dimer III shown in Figure 6c is comparable with dimer I in structure and binding strength as expected by the similar nature of the accepting oxygen. However, this oxygen atom is a bifurcated HB acceptor making it more negatively charged ($-0.58e$) compared to that of the accepting oxygen in dimer I ($-0.50e$), which gives rise to the slightly stronger binding in dimer III. Furthermore, with many binding sites available in the sulfonic acid group, several trimer conformations have been constructed as well as a tetramer structure, thus allowing investigation of binding methane in higher ratios of methane to ligand. Trimer I, combining the structure of dimers I and III, has been used to investigate the effect of binding methane in a 2:1 ratio (Figure 6d). It is shown that both individual dimer interactions have been strengthened upon forming the trimer. The interaction at the bifurcated HB acceptor oxygen (left) involves a charge increase at methane upon binding in the complex of $+12.8 \text{ me}$ and that at the other methane (right) of $+5.50 \text{ me}$. Other examples of methane binding in a 2:1 ratio are shown in trimer II, formed by superimposing dimers II and III (Figure 6e) and trimer III, which involves a combination of dimers I and II (Figure 6f). In these complexes, the binding energies have also been found to strengthen at both HB sites with respect to the corresponding dimer structures. The interactions are directional and typical of weak HB interactions. The sum of the binding energies found in each of the trimers are very similar. Combining the three dimers further gave a promising tetramer complex with three strong, directional HB interactions and short intermolecular distances (Figure 6g). The $O_{(OH)} \cdots H_{(CH_4)}$ and $O_{(S=O)} \cdots H_{(CH_4)}$ interactions strengthened relative to the corresponding dimers allow us to conclude that introduction of more methane molecules to the dimer complex is favorable. This could be a very powerful route to efficient capture of methane at increased pressures.

Figure 7 shows the methane complexes formed with phenylphosphonic acid. As with the sulfonic acid group, there are three available oxygen atoms for binding methane and so there are many dimer and trimer arrangements that can be formed, as well as a tetramer complex. Both dimers I and II (Figure 7a,b) only show weakly directional interactions but the binding energies are strong compared to all other functional groups investigated. Neither dimer gets stabilized via a weak hydrogen bonding interaction, judging by the optimized geometries of the dimers. The dimer I configuration of phenylphosphonic acid and methane displays the methane in close proximity with the functional group and the binding energy is the largest found for any dimer tested at $-5.93 \text{ kJ mol}^{-1}$. Dimer II, although binding methane strongly (the binding energy of this complex is $-4.07 \text{ kJ mol}^{-1}$), is

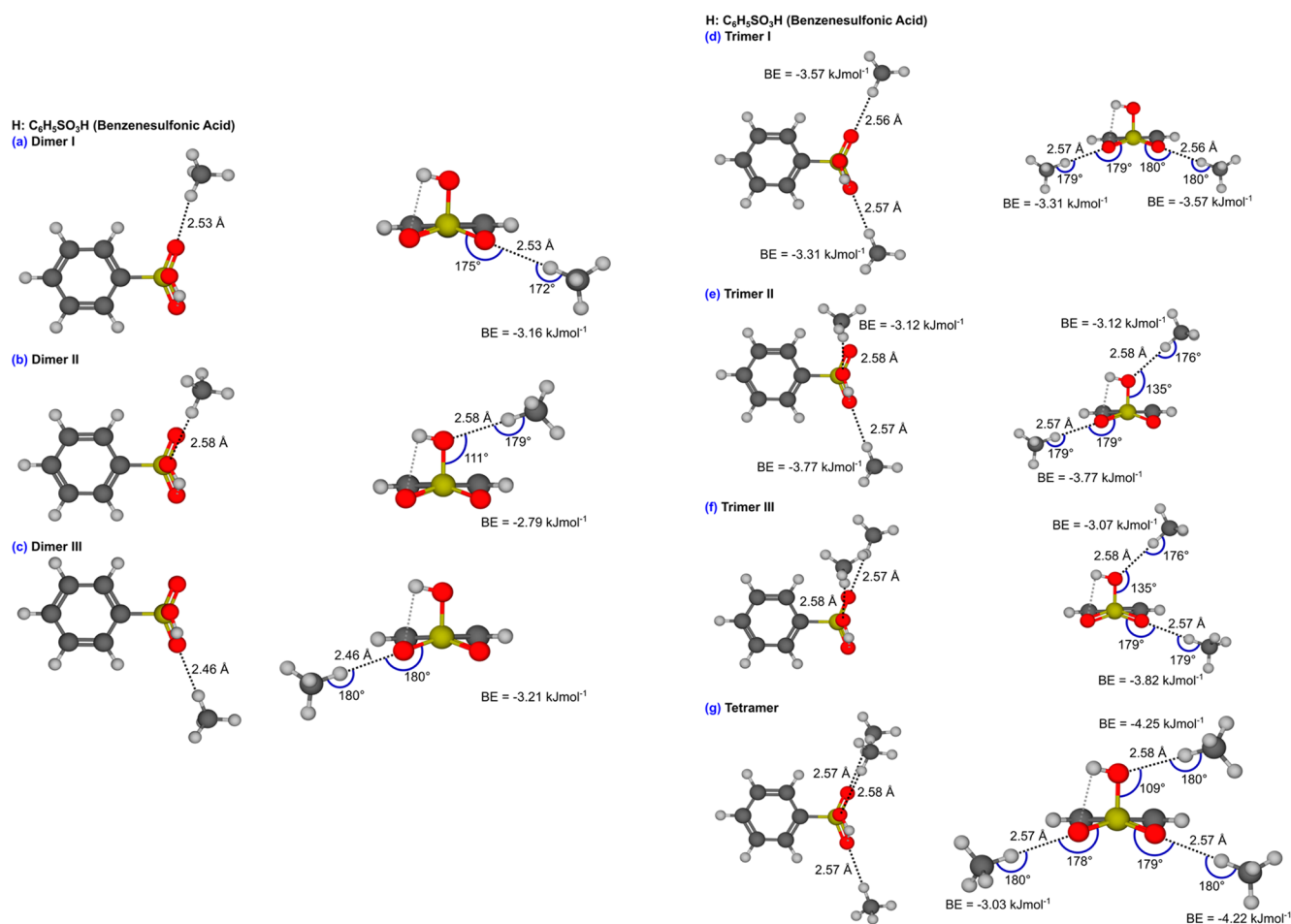


Figure 6. C₆H₅SO₃H (benzenesulfonic acid)–CH₄ complexes. Dimer structures (a)–(c) with methane molecules interacting directly with available oxygen sites. The atoms shown in gray, white, yellow, and red represent carbon, hydrogen, sulfur and oxygen, respectively. Trimers showing a combined structure of (d) dimers I and III, (e) dimers II and III and (f) dimers I and II. In complexes (d)–(f), the binding energies are stronger at both HB sites with respect to the corresponding dimer structures. (g) Tetramer complex combining the three dimers shows strong, directional HB interactions.

particularly inefficient in the way it binds to two O_(OH) binding sites which in principle, could be occupied by several methane molecules to form a trimer (as in the case of trimer I) or even a tetramer. The binding energies at these O_(OH) sites are greater when absorbing two or three methane molecules per organic linker. Dimer III (Figure 7c) shows a strong, directional interaction between the methane and the O_(P=O) atom that is stabilized by a weak HB with a short intermolecular distance of 2.44 Å. The binding was accompanied by a charge increase at the methane of +22.0 me. Dimer IV shows a strong binding site where the C–H bond of methane points to the lone pair of the accepting O_(OH) atom with an intermolecular distance of 2.53 Å (Figure 7d). Due to the symmetry of the functionalized benzene molecule, there exists an identical O_(OH) atom accepting site.

As with the benzenesulfonic acid, several trimers were tested to investigate the effectiveness of binding more methane molecules upon each linker. Trimer I involves methane molecules binding to each O_(OH) atom similarly to dimer IV but with stronger interactions. There is a slight asymmetry to the configuration as displayed by the angles, distances, and the resulting binding energies shown in Figure 7e. Trimer II (Figure 7f) is a combination of dimers III and IV in which the binding energy is strengthened slightly, giving moderately

strong interactions of –3.99 and –4.42 kJ mol^{–1} at the O_(P=O) site and O_(P–OH) site, respectively. Both interactions are highly directional and so are typical of weak hydrogen bonds. The final trimer tested is a combination of dimers II and III with a directional, weak HB-like interaction at the O_(P=O) site. The second methane molecule binds to both O_(P–OH) sites below the functional group as shown in Figure 7g. Both interactions are of significant strength yet methane binds more strongly within trimer I and, within the tetramer, methane binds both more strongly and more efficiently. The strongest interactions were found in the C₆H₅PO₃H···(CH₄)₃ tetramer shown in Figure 7h with very large binding energies and short intermolecular distances. Each of the C–H···O_(OH) angles is slightly distorted from the optimized angle of 180° found in the corresponding dimers. This is expected to be due to the steric repulsion between the methane molecules. Charge increases at the methane molecules of +1.46, +2.26, and +2.72 me were calculated corresponding to the binding energies of –6.21, –4.05, and –6.17 kJ mol^{–1}, respectively. Combining strong binding sites with a high methane to functional group ratio, the tetramer complexes of benzenesulfonic acid and phenylphosphonic acid demonstrate that these functional groups exhibit significant potential for enhanced CH₄ binding. The increased strength of hydrogen bond is caused by the

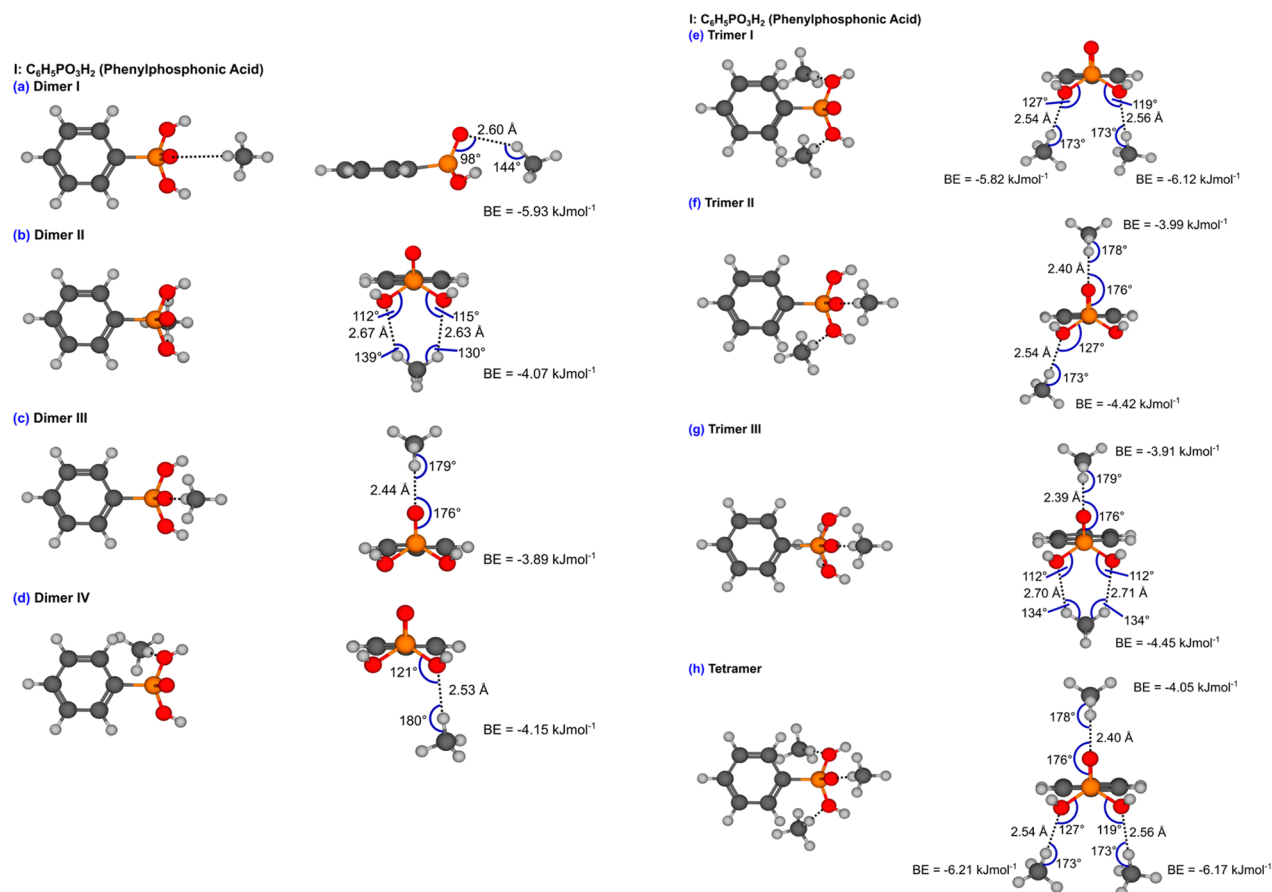


Figure 7. $C_6H_5PO_3H_2$ (phenylphosphonic acid)– CH_4 complexes. Dimer structures (a)–(d) with methane molecules interacting directly with one or both oxygen sites. The atoms shown in gray, white, orange, and red represent carbon, hydrogen, phosphorus, and oxygen, respectively. (e) Trimer I with methane molecules binding to each $O_{(OH)}$ atom similar to dimer IV but with stronger interactions. Trimers showing a combined structure of (f) dimers III and IV and (g) dimers II and III. (h) Tetramer complex showing the strongest interaction sites and hence a great potential for methane capture.

cooperative effect of many-body forces, and their association is more favorable than independent pairwise interactions.

The interactions of the dimer complexes compare well with results of similar studies. Research by Yu and co-workers focuses on the separation of CO_2 from CH_4 in membrane materials with studies of functional groups bonded to hexane and their interactions with methane compared to carbon dioxide at the same level of theory.²⁹ Three of the functional groups, $R-COOH$, $R-SO_3H$, and $R-PO_3H$, show similar dimer interactions with methane compared to our work, illustrating a consistency in result and how this work can be applied to other porous materials. However, the use of the aromatic groups seems to have an effect, particularly with the $R-OOH$ group in which the results differ most significantly, indicating the base structure has an impact on the overall interaction and needs to be taken into consideration.

Overall, the dimer complexes show significant HB character toward the oxygen atom lone pair from intermolecular distances and directional geometries. There is no general trend for carbonyl containing linkers being superior in their methane sorption ability than hydroxyl containing linkers. There is no clear trend between the binding energy and charge increase at the methane, suggesting that the interaction cannot be explained simply on a basis of charge on the methane as the dipole–dipole interaction within a HB is more complex. As seen in the Table 3, the charge at the hydrogen atom of the

methane is always more positive than that of the adjacent carbon atom, fitting well with the requirements for a hydrogen bond.

CONCLUSIONS

The lowest energy configurations and the associated binding energies were calculated for ligand–methane complexes involving nine different functional organic groups. It has been demonstrated that some organic molecules contain several binding sites available for various dimer, trimer, and tetramer conformations with the methane molecule. Although the dipole across the C–H bond in methane is relatively weak, the methane can bind via hydrogen bonding by accepting species such as carbonyl oxygen atoms. Each of the calculated energies gained from forming the dimers was enough to surpass RT (at room temperature). The $Ph-PO_3H_2$ ligand was the most encouraging candidate tested for binding methane via hydrogen bonding; the strongest binding energy calculated resulted from the $O_{(OH)} \cdots H_{CH_4}$ interaction of the $[Ph-PO_3H_2 \cdots CH_4]$ dimer. The phosphonic acid group also gave promising results upon introducing more methane molecules with the $[Ph-PO_3H_2 \cdots (CH_4)_3]$ tetramer, exhibiting the greatest binding energies calculated overall, suggesting binding in methane to ligand ratios of greater than 1:1 is feasible and can even be preferable. This could aid with sorption of methane at higher pressures.

Table 3. Dimer Complexes Listed in Order of Increasing Binding Strength with the Corresponding Atomic Charges of Carbon, Q_C , and Hydrogen, Q_H , As Determined by CHELPG Charge Analysis^a

label	dimer	binding energy, kJ mol ⁻¹	Q_C , me	Q_H , me
F	C ₆ H ₅ —OOH dimer II: H—O—H—CH ₃	-2.66	-0.48	0.15
H	C ₆ H ₅ —SO ₃ H dimer II: H—O—H—CH ₃	-2.79	-0.50	0.15
D	C ₆ H ₅ —COOH dimer II: H—O—H—CH ₃	-2.89	-0.48	0.14
G	C ₁₀ H ₆ O ₂	-3.06	-0.49	0.15
C	C ₆ H ₁₁ =O	-3.14	-0.50	0.17
H	C ₆ H ₅ —SO ₃ H dimer I: S=O—H—CH ₃	-3.16	-0.50	0.16
A	C ₆ H ₅ OH	-3.17	-0.50	0.16
H	C ₆ H ₅ —SO ₃ H dimer III: S=O(-H)—H— CH ₃	-3.21	-0.53	0.19
B	C ₆ H ₅ —C(=O)—H	-3.32	-0.46	0.14
F	C ₆ H ₅ —OOH dimer I: C—O—H—CH ₃	-3.54	-0.45	0.11
E	C ₆ H ₅ —NO ₂	-3.65	-0.52	0.17
D	C ₆ H ₅ —COOH dimer I: C=O—H—CH ₃	-3.75	-0.49	0.16
I	C ₆ H ₅ —PO ₃ H ₂ dimer III: P=O—H—CH ₃	-3.89	-0.57	0.23
I	C ₆ H ₅ —PO ₃ H ₂ dimer IV: H—O—H—CH ₃	-4.15	-0.50	0.16

^aDimers I and II of the phenylphosphonic acid (I) linker have been excluded as they do not show clear hydrogen bonding character.

The geometries found gave intermolecular (O⋯H_{CH₃}) distances similar to, or shorter than, the sum of the van der Waals radii, reinforcing the claim of weak hydrogen bonding interactions. It was also found that the C—H bond of methane generally directs toward the lone pair of the accepting oxygen, symptomatic of hydrogen bonding character. The investigations of trimers and tetramers were particularly promising with binding energies among the highest calculated through the study and the increase in methane to linker ratio causing methane to bind more efficiently.

The functional organic molecules selected in this work can be potentially incorporated into porous structures for enhanced methane capture. There are many examples of metal–organic frameworks containing phenol groups on their backbones³⁰ as well as —NO₂³¹ and —COOH³² groups incorporated in the pore. Considerably high methane uptakes have already been achieved in porous materials having —OH and —COOH groups attached to benzene in the organic linker.^{33,34} The carboxylate group has been widely used for the construction of stable porous structures due to its strong coordination ability to metal ions.³⁵ Although sulfonic and phosphoric acid groups can bind strongly to metal ions, the free forms of these functional groups can still be inserted in metal–organic frameworks by using carboxylate linkers with highly charged metal ions such as Zr(IV) or Hf(IV).³⁶

A weak interaction between an aliphatic C—H group and an aromatic π system plays a vital role in molecular recognition for numerous ligand-binding proteins. The interaction has also been used in drug design to increase the inhibitory activity and

selectivity. Furthering the understanding of these interactions and quantifying their energetics will have an important influence on the above applications.

AUTHOR INFORMATION

Corresponding Author

*Elena Besley. E-mail: Elena.Besley@nottingham.ac.uk. Tel: +44 115 846 8465.

Author Contributions

The manuscript was written through contributions of all authors. All authors have given approval to the final version of the manuscript.

Notes

The authors declare no competing financial interest.

ACKNOWLEDGMENTS

We thank the EPSRC and the University of Nottingham for funding. We acknowledge the High Performance Computing (HPC) Facility at the University of Nottingham for providing computational time. E.B. acknowledges an ERC Consolidator Grant for financial support. We are grateful to Drs. M. Suyetin, M. Lennox, and Y. Yang for fruitful discussions.

REFERENCES

- (1) Pucker, J.; Zwart, R.; Jungmeier, G. Greenhouse Gas and Energy Analysis of Substitute Natural Gas from Biomass for Space Heat. *Biomass Bioenergy* **2012**, *38*, 95–101.
- (2) Makal, T. A.; Li, J.-R.; Lu, W.; Zhou, H.-C. Methane Storage in Advanced Porous Materials. *Chem. Soc. Rev.* **2012**, *41*, 7761–7779.
- (3) Konstas, K.; Osl, T.; Yang, Y.; Batten, M.; Burke, N.; Hill, A. J.; Hill, M. R. Methane Storage in Metal Organic Frameworks. *J. Mater. Chem.* **2012**, *22*, 16698–16708.
- (4) Peng, Y.; Krungleviciute, V.; Eryazici, I.; Hupp, J. T.; Farha, O. K.; Yildirim, T. Methane Storage in Metal-Organic Frameworks: Current Records, Surprise Findings, and Challenges. *J. Am. Chem. Soc.* **2013**, *135*, 11887–11894.
- (5) Mason, J. A.; Veenstra, M.; Long, J. R. Evaluating Metal–organic Frameworks for Natural Gas Storage. *Chem. Sci.* **2014**, *5*, 32–51.
- (6) Eddaoudi, M.; Kim, J.; Rosi, N.; Vodak, D.; Wachter, J.; O’Keeffe, M.; Yaghi, O. M. Systematic Design of Pore Size and Functionality in Isoreticular MOFs and Their Application in Methane Storage. *Science* **2002**, *295*, 469–472.
- (7) Wang, X. Sen; Shengqian, M.; Rauch, K.; Simmons, J. M.; Yuan, D.; Wang, X.; Yildirim, T.; Cole, W. C.; López, J. J.; De Meijere, A.; et al. Metal-Organic Frameworks Based on Double-Bond-Coupled Di-Isophthalate Linkers with High Hydrogen and Methane Uptakes. *Chem. Mater.* **2008**, *20*, 3145–3152.
- (8) Ma, S.; Sun, D.; Simmons, J. M.; Collier, C. D.; Yuan, D.; Zhou, H. C. Metal-Organic Framework from an Anthracene Derivative Containing Nanoscopic Cages Exhibiting High Methane Uptake. *J. Am. Chem. Soc.* **2008**, *130*, 1012–1016.
- (9) Peng, Y.; Srinivas, G.; Wilmer, C. E.; Eryazici, I.; Snurr, R. Q.; Hupp, J. T.; Yildirim, T.; Farha, O. K. Simultaneously High Gravimetric and Volumetric Methane Uptake Characteristics of the Metal-Organic Framework NU-111. *Chem. Commun.* **2013**, *49*, 2992–2994.
- (10) Düren, T.; Sarkisov, L.; Yaghi, O. M.; Snurr, R. Q. Design of New Materials for Methane Storage. *Langmuir* **2004**, *20*, 2683–2689.
- (11) Torrisi, A.; Mellot-Draznieks, C.; Bell, R. G. Impact of Ligands on CO₂ Adsorption in Metal-Organic Frameworks: First Principles Study of the Interaction of CO₂ with Functionalized Benzenes. I. Inductive Effects on the Aromatic Ring. *J. Chem. Phys.* **2009**, *130*, 194703.
- (12) Torrisi, A.; Mellot-Draznieks, C.; Bell, R. G. Impact of Ligands on CO₂ Adsorption in Metal-Organic Frameworks: First Principles Study of the Interaction of CO₂ with Functionalized Benzenes. II.

Effect of Polar and Acidic Substituents. *J. Chem. Phys.* **2010**, *132*, 044705.

(13) Alsmail, N. H.; Suyetin, M.; Yan, Y.; Cabot, R.; Krap, C. P.; Lü, J.; Easun, T. L.; Bichoutskaia, E.; Lewis, W.; Blake, A. J.; et al. Analysis of High and Selective Uptake of CO₂ in an Oxamide-Containing {Cu₂(OOCR)₄}-Based Metal-Organic Framework. *Chem. - Eur. J.* **2014**, *20*, 7317–7324.

(14) Kim, K. C.; Yu, D.; Snurr, R. Q. Computational Screening of Functional Groups for Ammonia Capture in Metal-Organic Frameworks. *Langmuir* **2013**, *29*, 1446–1456.

(15) Grande, C. A.; Araujo, J. D. P.; Cavenati, S.; Firpo, N.; Basaldella, E.; Rodrigues, A. E. New π -Complexation Adsorbents for Propane–Propylene Separation. *Langmuir* **2004**, *20*, 5291–5297.

(16) Desiraju, G. R.; Steiner, T. *The Weak Hydrogen Bond: In Structural Chemistry and Biology*; IUCr monographs on crystallography; Oxford University Press: Oxford, U.K., 1999.

(17) Perry, J. J.; Perman, J. A.; Zaworotko, M. J. Design and Synthesis of Metal-Organic Frameworks Using Metal-Organic Polyhedra as Supermolecular Building Blocks. *Chem. Soc. Rev.* **2009**, *38*, 1400–1417.

(18) Nishio, M. CH/ π Hydrogen Bonds in Crystals. *CrystEngComm* **2004**, *6*, 130.

(19) Ribas, J.; Cubero, E.; Luque, F. J.; Orozco, M. Theoretical Study of Alkyl- π and Aryl- π Interactions. Reconciling Theory and Experiment. *J. Org. Chem.* **2002**, *67*, 7057–7065.

(20) Takahashi, O.; Kohno, Y.; Saito, K.; Nishio, M. Prevalence of the Alkyl/phenyl-Folded Conformation in Benzylic Compounds C₆H₅CH₂-X-R (X = O, CH₂, CO, S, SO, SO₂): Significance of the CH/ π Interaction as Evidenced by High-Level Ab Initio MO Calculations. *Chem. - Eur. J.* **2003**, *9*, 756–762.

(21) Sodupe, M.; Rios, R.; Nicholas, T.; Oliva, A.; Dannenberg, J. J. A Theoretical Study of the Endo/Exo Selectivity of the Diels-Alder Reaction between Cyclopropene and Butadiene. *J. Am. Chem. Soc.* **1997**, *119*, 4232–4238.

(22) Ujaque, G.; Lee, P. S.; Houk, K. N.; Hentemann, M. F.; Danishefsky, S. J. The Origin of Endo Stereoselectivity in the Hetero-Diels-Alder Reactions of Aldehydes with Ortho-Xylylenes: CH- π , π - π , and Steric Effects on Stereoselectivity. *Chem. - Eur. J.* **2002**, *8*, 3423–3430.

(23) Samanta, U.; Chakrabarti, P.; Chandrasekhar, J. Ab Initio Study of Energetics of X-H... π (X = N, O, and C) Interactions Involving a Heteroaromatic Ring. *J. Phys. Chem. A* **1998**, *102*, 8964–8969.

(24) Re, S.; Nagase, S. How Is the CH/ π Interaction Important for Molecular Recognition? *Chem. Commun.* **2004**, *6*, 658–659.

(25) Ringer, A. L.; Figs, M. S.; Sinnokrot, M. O.; Sherrill, C. D. Aliphatic C-H/ π Interactions: Methane - Benzene, Methane - Phenol, and Methane - Indole Complexes. *J. Phys. Chem. A* **2006**, *110*, 10822–10828.

(26) Shao, Y.; Molnar, L. F.; Jung, Y.; Kussmann, J.; Ochsenfeld, C.; Brown, S. T.; Gilbert, A. T. B.; Slipchenko, L. V.; Levchenko, S. V.; O'Neill, D. P.; et al. Advances in Methods and Algorithms in a Modern Quantum Chemistry Program Package. *Phys. Chem. Chem. Phys.* **2006**, *8*, 3172–3191.

(27) Boys, S. F.; Bernardi, F. The Calculation of Small Molecular Interactions by the Differences of Separate Total Energies. Some Procedures with Reduced Errors. *Mol. Phys.* **1970**, *19*, 553–566.

(28) Breneman, C. M.; Wiberg, K. B. Determining Atom-Centered Monopoles from Molecular Electrostatic Potentials. The Need for High Sampling Density in Formamide Conformational Analysis. *J. Comput. Chem.* **1990**, *11*, 361–373.

(29) Yu, D.; Matteucci, S.; Stangland, E.; Calverley, E.; Wegener, H.; Anaya, D. Quantum Chemistry Calculation and Experimental Study of CO₂/CH₄ and Functional Group Interactions for the Design of Solubility Selective Membrane Materials. *J. Membr. Sci.* **2013**, *441*, 137–147.

(30) Mo, K.; Yang, Y.; Cui, Y. A Homochiral Metal - Organic Framework as an Efficient Asymmetric Catalyst for Cyanohydrin Synthesis. *J. Am. Chem. Soc.* **2014**, *136*, 1746–1749.

(31) Zhang, Y.-B.; Furukawa, H.; Ko, N.; Nie, W.; Park, H. J.; Okajima, S.; Cordova, K. E.; Deng, H.; Kim, J.; Yaghi, O. M. Introduction of Functionality, Selection of Topology, and Enhancement of Gas Adsorption in Multivariate Metal–Organic Framework-177. *J. Am. Chem. Soc.* **2015**, *137*, 2641–2650.

(32) Eubank, J. F.; Mouttaki, H.; Cairns, A. J.; Belmabkhout, Y.; Wojtas, L.; Luebke, R.; Alkordi, M.; Eddaoudi, M. The Quest for Modular Nanocages: Tbo-MOF as an Archetype for Mutual Substitution, Functionalization, and Expansion of Quadrangular Pillar Building Blocks. *J. Am. Chem. Soc.* **2011**, *133*, 14204–14207.

(33) Rana, M. K.; Koh, H. S.; Zuberi, H.; Siegel, D. J. Methane Storage in Metal-Substituted Metal–Organic Frameworks: Thermodynamics, Usable Capacity, and the Impact of Enhanced Binding Sites. *J. Phys. Chem. C* **2014**, *118*, 2929–2942.

(34) Koh, H. S.; Rana, M. K.; Wong-Foy, A. G.; Siegel, D. J. Predicting Methane Storage in Open-Metal-Site Metal–Organic Frameworks. *J. Phys. Chem. C* **2015**, *119*, 13451–13458.

(35) Yan, Y.; Yang, S.; Blake, A. J.; Schröder, M. Studies on Metal-Organic Frameworks of Cu(II) with Isophthalate Linkers for Hydrogen Storage. *Acc. Chem. Res.* **2014**, *47*, 296–307.

(36) Choi, K. M.; Na, K.; Somorjai, G. A.; Yaghi, O. M. Chemical Environment Control and Enhanced Catalytic Performance of Platinum Nanoparticles Embedded in Nanocrystalline Metal–Organic Frameworks. *J. Am. Chem. Soc.* **2015**, *137*, 7810–7816.